Journal of Ginseng Research 47 (2023) 54–64

Contents lists available at ScienceDirect

Journal of Ginseng Research

journal homepage: https://www.sciencedirect.com/journal/journal-of-ginseng-research

Research Article

Microbiota, co-metabolites, and network pharmacology reveal the alteration of the ginsenoside fraction on inflammatory bowel disease

Dandan Wang [a, 1], Mingkun Guo [a, 1], Xiangyan Li [b], Daqing Zhao [b, *], Mingxing Wang [a, **]

[a] Research Center of Traditional Chinese Medicine, Affiliated Hospital, Changchun University of Chinese Medicine, Changchun, China
[b] Jilin Ginseng Academy, Changchun University of Chinese Medicine, Changchun, China

ARTICLE INFO

Article history:
Received 5 May 2021
Received in revised form
17 January 2022
Accepted 11 April 2022
Available online 18 April 2022

Keywords:
Ginsenoside
Microbiota
Co-metabolites
Network pharmacology
IBD

ABSTRACT

Background: Panax ginseng Meyer (P. ginseng) is a traditional natural/herbal medicine. The amelioration on inflammatory bowel disease (IBD) activity rely mainly on its main active ingredients that are referred to as ginsenosides. However, the current literature on gut microbiota, gut microbiota-host co-metabolites, and systems pharmacology has no studies investigating the effects of ginsenoside on IBD.
Methods: The present study was aimed to investigate the role of ginsenosides and the possible underlying mechanisms in the treatment of IBD in an acetic acid-induced rat model by integrating metagenomics, metabolomics, and complex biological networks analysis. In the study ten ginsenosides in the ginsenoside fraction (GS) were identified using Q-Orbitrap LC-MS.
Results: The results demonstrated the improvement effect of GS on IBD and the regulation effect of ginsenosides on gut microbiota and its co-metabolites. It was revealed that 7 endogenous metabolites, including acetic acid, butyric acid, citric acid, tryptophan, histidine, alanine, and glutathione, could be utilized as significant biomarkers of GS in the treatment of IBD. Furthermore, the biological network studies revealed EGFR, STAT3, and AKT1, which belong mainly to the glycolysis and pentose phosphate pathways, as the potential targets for GS for intervening in IBD.
Conclusion: These findings indicated that the combination of genomics, metabolomics, and biological network analysis could assist in elucidating the possible mechanism underlying the role of ginsenosides in alleviating inflammatory bowel disease and thereby reveal the pathological process of ginsenosides in IBD treatment through the regulation of the disordered host–flora co-metabolism pathway.

1. Introduction

Inflammatory bowel disease (IBD) represents a group of chronic inflammatory conditions with an unknown etiology, including ulcerative colitis (UC) and Crohn's disease (CD). The incidence of IBD worldwide is increasing every year [1]. The current literature suggests that an imbalance in the intestinal microbiota could be the inducing factor for IBD, although the underlying mechanism remains unclear so far [2].

Gut microbiota, in addition to assisting in nutrient metabolism, participates in and influences the host metabolism and thus has a co-metabolism relationship with the host [3]. Several natural products are digested and absorbed throughout the gastrointestinal tract, which generates a variety of small molecule metabolites, such as short-chain fatty acids, trimethylamine, bile acids, indoles, phenols, benzoic acids, polyamines, vitamins, etc., which are referred to as co-metabolites [4]. These co-metabolites play an important role in maintaining the intestinal environment and host health. Therefore, the gut microbiota is closely associated with the efficacy of natural medicine, and the regulation of gut microbiota structure and metabolite differences could serve as the target for natural medicines.

P. ginseng is a perennial herb of *Araliaceae acanthopanax* that has been used for thousands of years in China, Japan, and Korea as traditional herbal medicine [5]. The chemical properties and pharmacological activities of P. ginseng have been studied extensively across the world. Ginsenosides, the main active compounds of

* Corresponding author. Jilin Ginseng Academy, Changchun University of Chinese Medicine, Changchun, 130021, China.
** Corresponding author. Research Center of Traditional Chinese Medicine, Affiliated Hospital, Changchun University of Chinese Medicine, Changchun, 130021, China.
E-mail addresses: zhaodaqing1963@163.com (D. Zhao), cc_wmx@163.com (M. Wang).
[1] The first two authors made equal contribution to this work.

https://doi.org/10.1016/j.jgr.2022.04.001

ginseng, exhibit several pharmacological effects, such as anti-inflammation, anti-tumor effect, regulation of the central nervous system, treatment of diabetes, among others [6,7]. In recent years, the pharmacological effects of ginseng and ginsenosides on IBD have been revealed. However, most of the reported studies focused on the changes in the number, proportion, and function of gut microbiota due to Ginseng usage, and the regulation mechanism of gut microbiota related to metabolites requires further investigation.

Therefore, in the present study, the anti-IBD activity of ginseng was investigated. After extracting the total ginsenosides extract, the composition of the ginsenosides extract was determined using LC-MS. Subsequently, using genomics and metabolomics methods, the gut microbiota and its host co-metabolites were analyzed in a rat model of acetic acid-induced acute enteritis. The anti-IBD activity of ginsenosides was evaluated using network pharmacology analysis and molecular docking. The findings of the present study would establish a foundation for future studies on deciphering the mechanism and novel targets of ginseng in IBD treatment.

2. Materials and methods

2.1. Chemicals and reagents

P. ginseng was purchased from Wudu County (Gansu Province, China). Standard ginsenosides Rk1, Rk3, Rg1, Rg2, Rg5, Rh1, Rh2, Rb3, Re, and PPD were all obtained from the National Institute for the Control of Pharmaceutical and Biological Products (Beijing, China). All chemicals used were of analytical grade unless otherwise specified. The anti-GAPDH, anti-EGFR antibodies were obtained from Boster biological technology (Wuhan, China). MEM culture medium were obtained from Cobioer County (Nanjing, China).

2.2. Preparation of ginsenosides fraction (GS)

Ginseng (500 g) was placed in 5, 4, and 3 L of boiling water for 2 h for the extraction of GS. The obtained extracts were filtered, mixed, and concentrated to 600 mL in a Rotary Evaporator at 60 °C. Next, the total ginsenoside was purified as described in a previous report [8]. In brief, 100 mL of the concentrated extract was applied to a column of macroporous adsorption resin (5 × 75 cm). First, the polysaccharides were completely eluted with water. Then, ethanol (90%) was applied to the column to elute the ginsenosides. The ethanol eluates were collected and freeze-dried.

2.3. Chromatography and mass spectrometry

2.3.1. Sample preparation

An appropriate amount of TG was mixed in methanol, and the mixture was then subjected to ultrasonic treatment for 30 min. The resultant sample was filtered using a 0.22-μM filter membrane and then injected for standby.

2.3.2. Preparation of the reference solution

In order to prepare 10 mg/mL of the mixed standard solution, appropriate amounts of the reference standards of the ginsenosides Rk1, Rk3, Rg1, Rg2, Rg5, Rh1, Rh2, Rb3, Re, and PPD were dissolved in methanol, followed by filtering the resultant mixture with 0.22-μM filter membrane prior to sample injection for standby.

2.3.3. Chromatographic conditions

LC analysis was performed using Ultimate 3000RS (Thermo-Fisher, USA). The separation of samples was achieved on an RP-C18 column (2.1 mm × 150 mm, 1.8 μm) at the temperature of 35 °C and a flow rate of 0.3 mL min^{-1}. The mobile phases A and B were ultrapure water and acetonitrile, respectively. The gradient eluent profile was as follows: 0–40 min, 18%–21% B; 40–42 min, 21%–26% B; 42–46 min, 26%–32% B; 46–66 min, 32%–33.8% B; 66–71 min, 33.8%–38% B; 71–78 min, 38%–49.1% B; 78–82 min, 49.1% B; 82–83 min, 49.1%–50.6% B; 83–88 min, 50.6%–59% B; 88–89.8 min, 59.6%–65% B; 89.8–97 min, 65% B; 97–102 min, 65%–85% B; 102–109 min, 85% B; and 109–141 min, 18% B. The real-time detection was performed at the wavelength of 256 nm. The injection volume of the samples was 2 μL.

2.3.4. Mass spectrometric condition

MS analysis was conducted using an Ion Trap Orbital Well Combined High-Resolution Mass Spectrometer (Instrument model: Q Exactive, Thermo Fisher), combined with an ESI ± ion source. The operation parameters were as follows: sheath gas, N2 (assay >99.999%), 40Arb; collision gas, high-purity helium; capillary temperature, 300 °C; Aux gas and heater temperature, N2 (assay >99.999%) and 350 °C; resolution, 17,500; spray voltage, 3.2 kV; analyzer, PRM; scan type, full. The scan range was m/z 50–500.

2.4. Rat model assessment

8-week-old SD rats (weighing 200–250 g each) were procured from the Jilin University College of Pharmacy, along with a health and safety certificate of conformity administered by the Chinese government (ShengChanXuKe number: SCXK2016–0001). The rats were housed in an SPF animal center (12-h light/12-h dark cycle, 23 ± 3 °C and 50% ± 10% relative humidity). All rats were acclimatized for 7 days prior to the experiments and subsequently divided randomly into three groups (5 males and 5 females each group): Healthy control, Model group, and GS group. The animal colitis model was established based on a previously reported protocol [3] and the experimental design illustrated in Fig. 2A. After weighing, the animals were anesthetized and killed. The distal 10 cm of the colon, measured through the insertion of a ballpoint syringe, was removed and opened by performing a longitudinal incision.

2.5. Tissue sample preparation and ELISA

The colonic tissues of 5 rats were randomly selected from each group and subjected to histopathological analysis after the fixing of the colon specimen in 10% formalin in PBS followed by embedding in paraffin. Approximately 4 mm-thick sections of the colon were prepared, stained with Eosin and Hematoxylin, and then observed under a light microscope. All sections were analyzed and interpreted by a certified histopathologist. The remaining colonic tissues were homogenized in a commercial Pro-Prep Protein Extraction Solution (Shanghai Beyotime, China). The relative parameters were determined using Elisa kits according to the manufacturer's instructions.

2.6. Collection of intestinal contents

Fecal samples were collected at baseline for all subjects and at 6-month and 12-month visits for the IBD patients only. The fecal samples were collected using sterile plastic tubes and then stored at −80 °C until analysis.

2.7. DNA extraction, PCR, and MiSeq sequencing

DNA was extracted from colon contents using the Omega Mag-Bind Soil DNA Kit (200) (Omega Bio-Tek, USA). Subsequently, the V3–V4 regions of the 16S rDNA were PCR amplified using the forward primer 338F 5′-ACTCCTACGGGAGGCAGCA-3′ and the reverse

primer 806R 5′-GGACTACHVGGGTWTCTAAT-3'. Sequences were annotated using the NT database. The amplicon library was then subjected to paired-end sequencing (2 × 250 bp) according to standard protocols on an Illumina MiSeq platform (Illumina, San Diego, USA). Chao, Shannon indices and analysis of bacterial abundant were determined using QIIME. The pictures were displayed using R language and ggplot2 package.

2.8. Host–microbial metabolism

2.8.1. Metabolite sample preparation

Untargeted metabolomics analysis was performed using previously reported sample preparation and MCF-based derivatization protocols with modifications [9,10]. A 1-μL aliquot from each derivatized sample was injected into a gas chromatography system coupled to a time-of-flight mass spectrometry (GC-TOFMS) system (Pegasus HT, Leco Corp., St. Joseph, MO, USA) and operating in the electron ionization (EI) mode. The Rxi-5MS column (30 m × 250 μm I.D., 0.25-μm film thickness, Crossbond ® 5% diphenyl/95% dimethyl polysiloxane) was used at the initial temperature of 45 °C for 1 min which was then increased at the rate of 20 °C/min to 260 °C, then to 320 °C at a rate of 40 °C/min, and maintained at this temperate for 2 min. The injector temperature was 270 °C. The ions were generated using a 70-eV electron beam, and the detector voltage was 1450 V. The gas flow rate through the column was 1 mL/min, and 20 spectra/s were recorded in the mass range of 38–550 *m/z*.

2.8.2. Data processing and statistical analysis

The raw metabolomics data generated from GC-TOFMS were processed for automatic baseline denoising, smoothing, peak selection, and peak signal alignment using the proprietary software XploreMET v2.0 (Metabo-Profile, Shanghai, China). Normalization to total mass concentrations of the metabolites (percentage) was performed to ensure that all subjects were directly comparable and to reduce the large biological variations in the samples. Multivariate statistical analyses, such as principal component analysis (PCA) and partial least square discriminant analysis (PLS-DA), along with univariate statistical analysis (ANOVA) and pathway analysis, were performed using MetaboAnalyst version 3.0 (http://www. metaboanalyst.ca). In order to evaluate the model and prevent the overfitting of the supervised model, 100-permutation cross-validation was performed. The metabolites with threshold |p [1]| greater than 2 in the OPLS-DA and the FC threshold greater than 1.2 or lower than 0.8 (P-value lower than 0.05) were selected as the potential important contributors to the group classifications and further subjected to metabolic pathways mapping using the Kyoto Encyclopedia of Genes and Genomes (KEGG) database for pathway enrichment.

2.9. Network pharmacology

2.9.1. Screening of drug targets and disease targets

The drug targets corresponding to ginsenosides were obtained from the TCMSP database (http://tcmspw.com/tcmsp.php) and the Swiss Target Prediction (probability >0) database. Subsequently, target screening was performed based on the P-value. Disease targets associated with IBD were obtained from the GeneCard database (https://www.genecards.org/). The disease targets were screened based on the obtained Relevance scores.

2.9.2. Construction of the compound–protein targets–disease network

The drug-target network was constructed by importing the names of the ginsenosides, drug targets, and diseases into the Cytoscape 3.7.2 software. In order to conduct research on the treatment of IBD using ginsenosides, the IBD-associated disease targets were matched with the drug targets of ginsenosides to obtain the intersection targets and construct a Venn diagram. Next, using the Cytoscape 3.7.2 software, a drugs–intersection targets–disease network was constructed. Then, using the Cyto NCA plug-in, a topological analysis of the drug–intersection targets–disease network was performed. On the basis of the Degree, Betweenness, and Closeness, the nodes were filtered, while the ginsenosides were arranged according to the Degree value.

2.9.3. GO and KEGG analysis of the intersection targets

Using the GO (Gene Ontology, http://www.geneontology.org/) and KEGG pathway (Kyoto Encyclopedia of Genes and Genom, http://www.genome.jp/kegg/) databases and a combination of calculations (GO, Count $\geq$2, P $\leq$ 0.05. KEGG, P $\leq$ 0.01), the biological reactions and pathways associated with the involved intersection targets were determined. The results were visualized, analyzed, and arranged according to the P-value. Using the Cytoscape 3.7.2 software, the intersection target–signaling pathway network and the intersection target–biological functions network diagrams were constructed.

2.10. Molecular docking

The target protein structures were obtained from the PDB database (https://www.rcsb.org/Category-search), and the 3D structures of the ginsenoside ligands were retrieved from the TCMSP platform (https://tcmspw.com/tcmsp.php). The small molecule structures and the water molecules within the target protein structure were deleted using Pymol 15 software. The charge of the target protein was calculated using the AutoDock software. The rotation bond and box of the ligand were determined, followed by performing rigid docking. The docking results were visualized and analyzed using the Pymol software.

2.11. EGFR target identification of ginsenoside Rk1 by cellular thermal shift assay (CETSA)

The human colon adenocarcinoma Caco-2 cell line was obtained from the Procell Life Science and Technology Company and was maintained in MEM with 10% FBS, 1% nonessential amino acids, and gentamicin (50 mg/mL) at 37 °C and 5% CO_2; the medium was replaced every two days. Then, CETSA was completed according to the reported method [11,12]. Briefly, the culture medium was seeded onto 6-well plates at a density of 5 × 10^5 cells/well. Caco-2 cells were fed with ginsenoside Rk1(40 μM, dissolved by DMSO) for 2 h. Caco-2 cells were digested by trypsin followed by resuspension in PBS (protease inhibitor). The cell suspension were aliquoted as sample. Then, each sample was heated at designated temperatures ranging from 48 to 60 °C for 3 min, followed by cooling for 3 min at room temperature. Each sample was separated by centrifuging at 12,000 r.p.m. for 25 min and then analyzed by Western blot.

2.12. Statistical analysis

All experiments were conducted in triplicate. The results were expressed as means ± standard deviation (SD). The obtained data were evaluated by performing a one-way analysis of variance using the SPSS 17.0 software (SPSS, Inc., Chicago, IL, USA). Differences between the groups were evaluated using the Student–Newman–Keuls (SNK) test. The significance threshold was set at P-value < 0.05.

3. Results

3.1. Composition analysis using LC-MS

When the LC-MS was operated in positive and negative ion scan mode, 5 kinds of negative ions (m/z = 800.49066, 946.54749, 622.44396, 620.42815, 1078.58398) and 5 kinds of positive ions (m/z = 784.49653, 752.47087, 460.39122, 624.36139, 766.48617) were obtained. The analysis and comparison of the retention times and molecular weights of the samples and the standard revealed the ginsenoside monomers from the total ginsenosides (Supplementary Table 1). The 10 ginsenosides monomers identified were: Rk1, Rk3, Rg1, Rg2, Rg5, Rh2, Rb3, Re, PPD, and Rh1. The m/z of the precursor ion of the sample was similar to the m/z of the 10 standards used. After analyzing the ion reference graph (Fig. 1A) obtained from the LC-MS analysis, the retention time of the sample was observed to be similar to the retention times of the 10 standard products. The decoction and the deduced structure formula for the ten ginsenosides are presented in Fig. 1B. The LC-MS analysis and the comparison of the retention times of the samples with those of the standards and the molecular weights determined using mass spectrometry confirmed the following ten components: Rk1 (0.9%), Rk3 (0.08%), Rg1 (2.95%), Rg2 (0.94%), Rg5 (0.85%), Rh1 (2.42%), Rh2 (0.13%), Rb3 (6.99%), Re (8.65%), and PPD (0.72%).

3.2. Histological and serological analyses

The typical symptoms of acetic acid-induced intestinal inflammation like IBD in rats, including weight loss, decreased food consumption, bloody stool, anus prolapse, dull hair and mental malaise were observed in the model group. After treatment with GS, weight and food consumption of rats in the GS group was increased. bloody stool, anus prolapse, dull hair and mental malaise were relieved. In addition, it was evident with the H&E staining that GP alleviated severe lesions in the colon tissue (Fig. 2B), such as those with the histopathological characteristics of mucosal damage, necrosis, and inflammatory infiltration, in the IBD rat model (Fig. 2B). Furthermore, the serological parameters, including IL-1β, IL-10, and TNF-α, were measured to investigate the therapeutic effects of GS (Fig. 2C). Both the proinflammatory cytokines, IL-1β and TNF-α, were increased in the rats with inflamed intestinal mucosa, although this effect could be restored with GS treatment. The IL-10 content exerted the opposite effect compared to IL-1β in the different groups. These results indicated that GS significantly ameliorated the colitis symptoms.

3.3. 16s-rRNA analysis

A simple analysis showed that ginsenosides are able to restore changes in gut microbiota induced by IBD, including increased Chao1 and Shanno (Fig. 2D). Meanwhile, PLS-DA indicated that the model group, control group and GS group had significant differences in bacterial composition (Fig. 2F). A detailed analysis revealed that 45 bacterial taxa exhibited significant differences among the different groups (Fig. 2G). Certain bacteria associated with ulcerative colitis are concerning. It should be noted that *Akkermansia* bacteria assist in maintaining the integrity of the intestinal mucosa and providing nutrients to the colonic mucosa [13]. Reduced *Akkermansia* abundance has been associated with a variety of intestinal diseases. In this study, the acetic acid treatment downregulated the abundance of *Akkermansia,* which was increased after the GS treatment. Furthermore, amino acid metabolism has emerged as a popular focus in ulcerative colitis research in recent years [9], with several amino acid metabolism-related bacterial taxa, such as *Peptostreptococcaceae, Jeotgalicoccus, Corynebacterium,* and *Coprococcus,* demonstrating significant differences between the acetic acid-induced and control groups. GS treatment could reverse these changes to different degrees. Among these taxa, *Corynebacterium* and *Coprococcus* abundances were significantly decreased after GS treatment, while the abundances of *Peptostreptococcaceae* and *Jeotgalicoccus* have rising trends after the GS intervention (Fig. 2E). PICRUSt was used to predict the 16S rRNA gene sequences in the KEGG Pathway Database (Fig. 2H). It could be observed from the data that the abundance of the bacteria associated with amino acid metabolism pathways was the highest, with certain differences among the groups. The results of the microflora analysis suggested that intestinal flora could be used as the target for GS to regulate the host metabolism. Therefore, based on the above results, the differences in the host co-metabolites were analyzed.

3.4. Microbiota-host co-metabolites analysis

3.4.1. Metabolic variation

PCA score plots that were drawn based on the data matrix of the control group, model group, and GS treatment group revealed the overall classification among the groups (Fig. 3A). Although a sample was clustered together with the model group, the tendency and the separations between the control and model groups were visible (p1 = 1.5e-02, p2 = 7e-03). In addition, there was an obvious classification between the model group and the GS treatment group (p1 = 0.085, p2 = 1e-02), while the samples from the control group and the GS treatment group were misclassified and clustered together (p1 = 1, p2 = 0.105). In order to further investigate the classification of the three groups, a supervised pattern recognition method (PLS-DA) was utilized (Fig. 3B). The distinction between the healthy control group and the model group was obvious, while the plots of the GS group were located together with the healthy control group. The metabolite profiling of these rats suggested that GS treatment shifted the metabolites from disease status to healthy status. Next, the major contributors to metabolite variation were analyzed to identify potential biomarkers for IBD and the targets for GS.

3.4.2. Major differentially expressed metabolites

The differentially expressed metabolites were mainly from the fatty acid and amino acid categories (Fig. 3C). All the important variables that contributed to the group classifications among the three groups were displayed in the Volcano plots using log10(p) and Log2(FC). A total of 23 metabolites were identified as the most important contributors, among which 19 metabolites were downregulated, and 4 metabolites were upregulated in the UC group compared to the healthy control group. As expected, treatment with GS reversed these alterations in most of the metabolites in the UC group. Details of the differential metabolites are provided in Table 1. Taken together, the results demonstrated elevated levels of amino acids in the UC group compared to the healthy controls. Conversely, short-chain fatty acids (SCFAs), butanoate in particular, were greatly decreased in the model rats compared to the healthy controls, with the GS intervention returning the levels of most of the SFCAs in the intestinal contents to normal ranges.

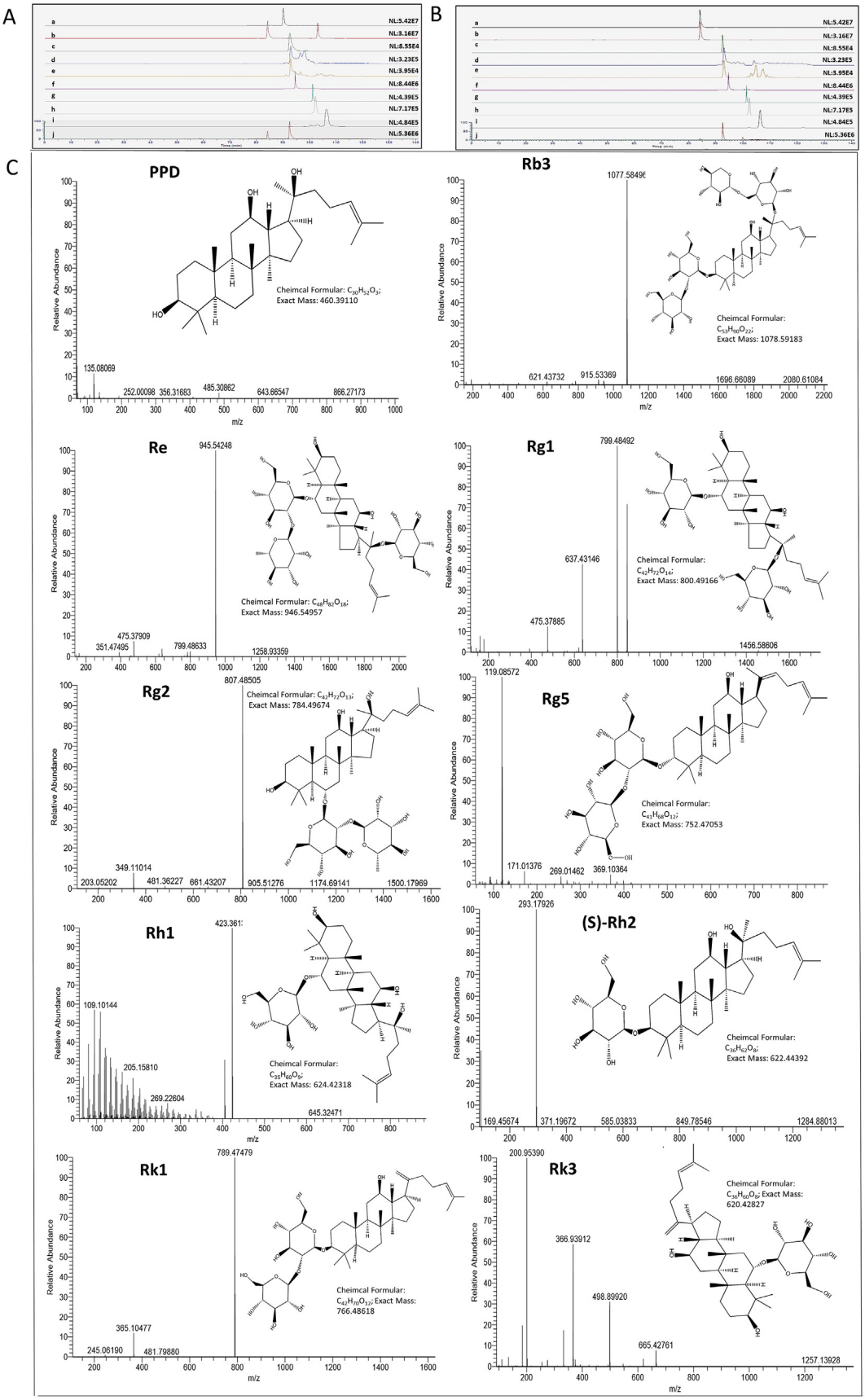

Fig. 1. LC-MS analysis of GS. (A and B). The ion current diagram of GS and references. (C). The mass spectrum of each peak in ion current diagram of GS and the deduced structure formula.

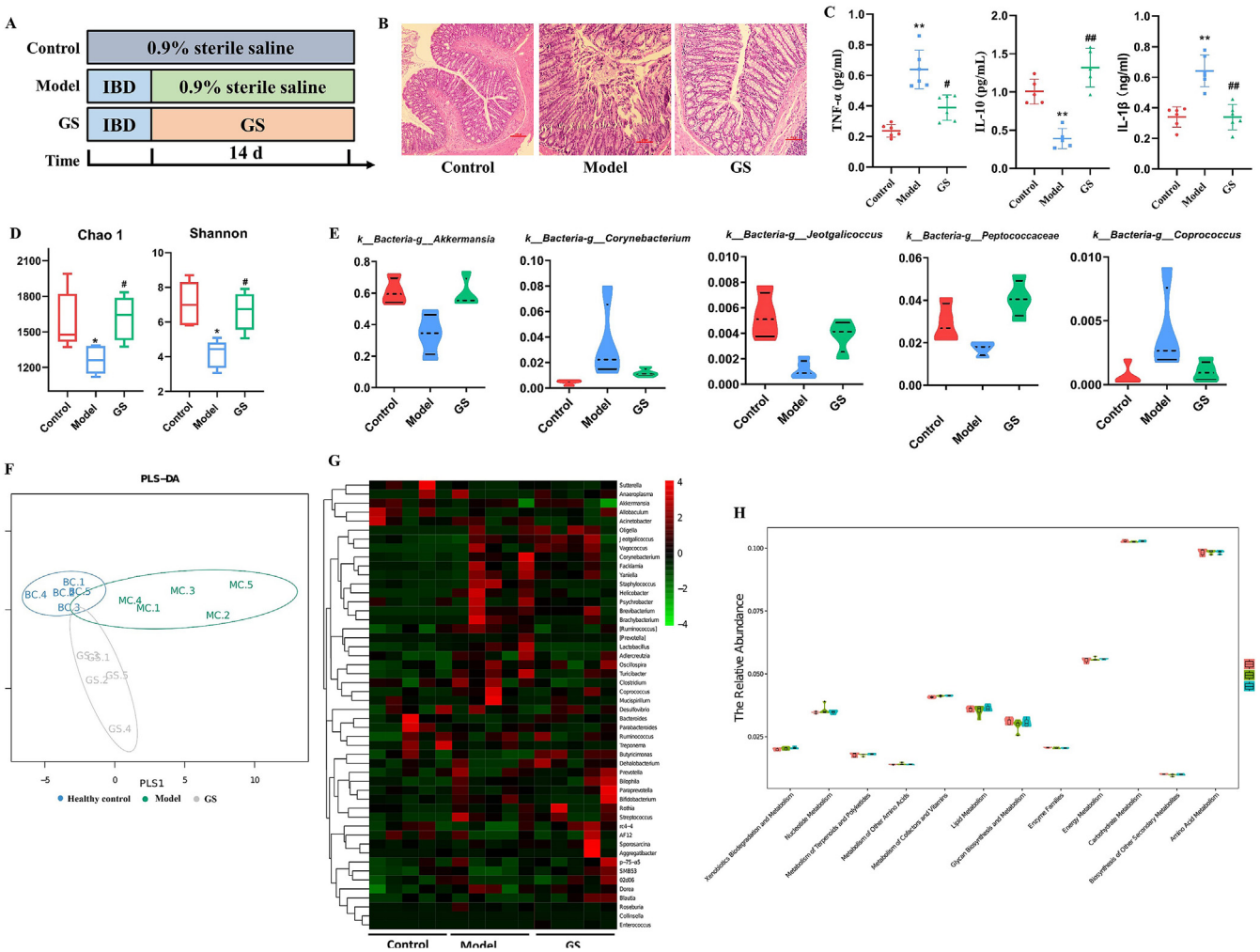

Fig. 2. The effects of GS on histological, serology and gut dysbiosis induced by acetic acid. (A) Scheme of experimental design. (B) H&E stained colon tissue (40 ×). (C) Cytokines levels in serum. (D) Chao1 and Shannon index. (E) Box plots of five significant differential bacteria. (F) PLS-DA score plot. (G) Heatmap of 40 bacterial species altered by acetic acid or GS. (H) Picrust predicts a second-rank KEGG distribution. *P < 0.05, **P < 0.01 VS Control group; #P < 0.05, ##P < 0.01 VS Model group.

3.4.3. Differential metabolites and other relevant pathways

To identify biologically relevant patterns based on the metabolomics data, QEA (quantitative enrichment analysis) was conducted for all three groups (Fig. 3E). The metabolic pathway analysis based on KEGG identified Butanoate, Nitrogen, Glyoxylate, and amino acid metabolisms, along with Citrate cycle and metabolism, to be significantly enriched, reinforcing that GS alleviates the intestinal inflammation partly by regulating the microbiota–host co-metabolism.

3.5. Network pharmacological analysis

3.5.1. Screening of drug targets and disease targets

A total of 9 ginsenoside targets (Rk1, Rk3, Rg1, Rg2, Rg5, Rh2, Rb3, Re, and PPD) were identified from the Swiss Target Prediction database and the TCMSP database (Rh1 Probability = 0, abandon). After screening, 112 protein targets were obtained. The GeneCards database provided 2804 disease targets (Relevance score >5.2) of inflammatory bowel disease. The disease targets were considered to be strongly related to IBD when the Relevance score was >5.2 (Fig. 4A).

3.5.2. Construction of the compound–protein target–disease network

The compound–protein target network was constructed using the protein targets of the ginsenosides Rk1, Rk3, Rg1, Rg2, Rg5, Rh2, Rb3, Re, and PPD (Fig. 4B). In order to further study the effect of treatment with ginsenosides in IBD, the IBD disease targets were matched with the protein targets of the above-stated 9 ginsenosides, which generated 92 intersection targets of the herbal medicine targets and the disease targets. The compound–intersection target network was then constructed using these 92 intersection targets. Cytoscape 3.7.2 was employed for visual analysis, as depicted in Fig. 4B. Certain ginsenosides had a greater number of intersection targets compared to other ginsenosides (Table 2). For instance, Rk3 had 63 intersection targets, Rk1 had 40 intersection targets, and Rg5 and Rh2 had 27 intersection targets each. The remaining ginsenosides had over 10 intersection targets each. It was revealed that the intersection target STAT3 was linked to 9 ginsenosides, VEGFR and IL2 were linked to 9 ginsenosides, and EGFR was linked to 6 ginsenosides. The remaining intersection targets connected 2 or more ginsenosides each. Using the Cyto NCA plug-in, ginsenosides were arranged according to their Degree value and the results are

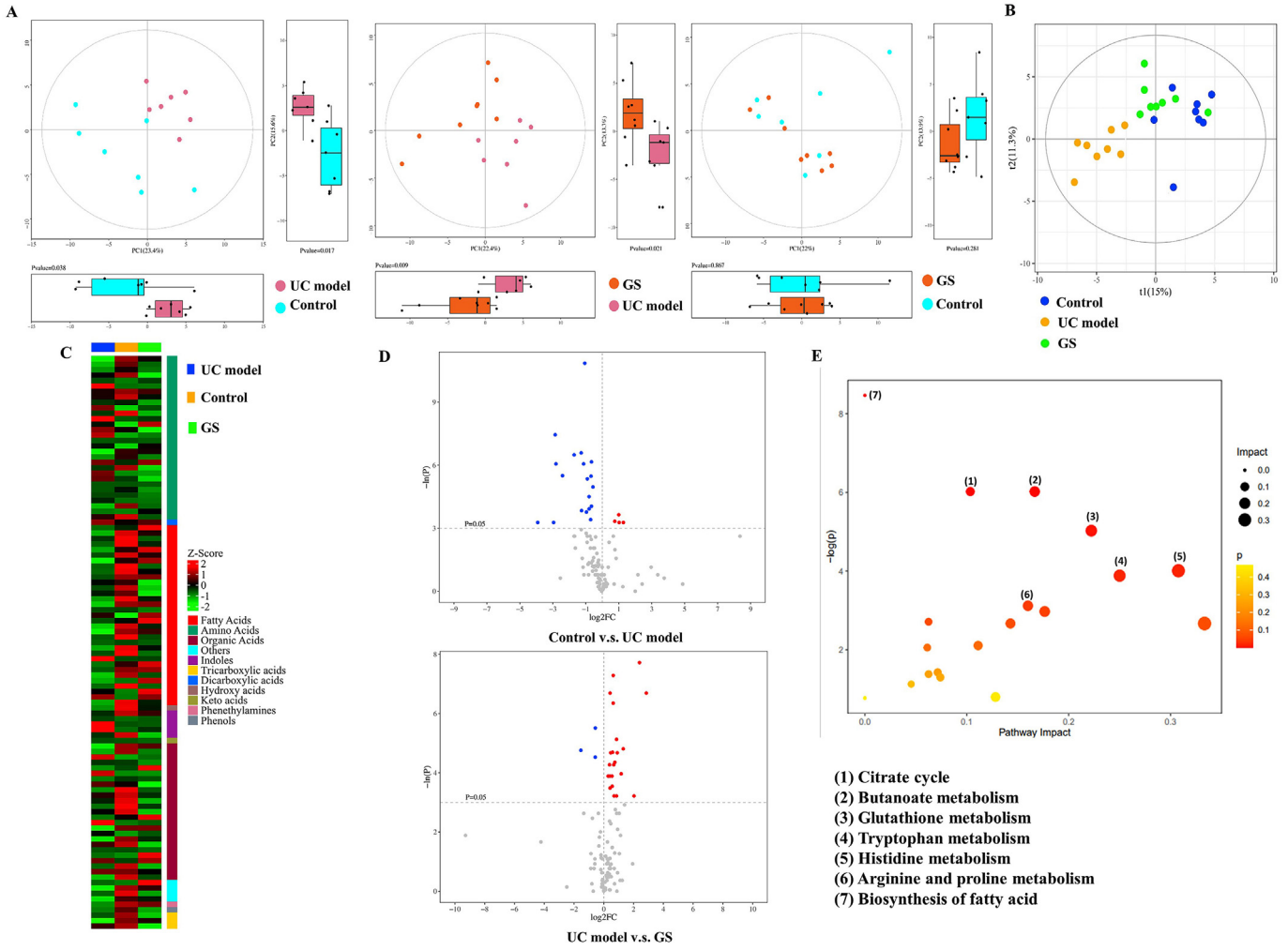

Fig. 3. The effects of GS on Microbiota-host co-metabolites. (A) PCA scores plot. (B) PLS-DA sores plot profiling of administration GS and acetic acid compared with control groups ($R^2X(cum) = 0.352$, $R^2Y(cum) = 0.856$, $Q^2(cum) = 0.332$). (C) Heatmap of differentially expressed metabolite contents. (D) Volcano plots for displaying of the important metabolites contributed to the group differences. (E) Pathway Analysis.

presented in the Supplementary Table 2. The Degree values of 4 ginsenosides, namely, Rk3, Rk1, Rg5, and Rh2, were relatively larger.

3.5.3. GO and KEGG analyses of the intersection targets

The GO database analysis ($P < 0.05$ as the reference standard) revealed 58 biological functions in the 92 intersection targets of the 9 ginsenosides. In order to facilitate intuitive comparison, the identified 58 biological functions were arranged according to the P-value. The GO analysis results are presented in Fig. 4C. The intersection targets were observed to be mainly involved in serine/threonine kinase activity, serine/threonine/tyrosine kinase binding, phosphatase binding, 1-phosphatidylinositol-3-kinase activity, phosphatidylinositol 3-kinase activity, and other biological functions. In the intersection target–biological functions network (Fig. 4B). On the basis of the P-value, the top 20 pathways were utilized to prepare a bar graph. EGFR was involved in 13 pathways, STAT3 was involved in 10 pathways, and AKT1 was involved in 8 pathways. The remaining targets were involved in 2 or more pathways each. Therefore, it was inferred that EGFR, STAT3, and AKT1 were the key intersection targets.

3.6. Active components in GS predicted to be potential targets using molecular docking

The above results revealed that EGFR, STAT3, and AKT1 participated in most of the pathways, indicating they were the most important protein targets. According to the Degree values of 4 ginsenosides in the "component–target–disease" network and the number of intersection targets, the main active components of GS were Rk1, Rk3, Rg5, and Rh2. These four ginsenosides were associated with the key intersection targets EGFR, STAT3, and AKT1. When the binding energy between the ligand and the receptor is less than -4.25 kcal mol^{-1}, the ligand and the receptor exhibit a certain binding activity. When the binding energy is less than -5.0 kcal mol^{-1}, there is better binding activity. The results of the docking of the 4 main ginsenosides with 3 target proteins are presented in the Supplementary Table 4. These four ginsenosides had weak binding activity with STAT3 and AKT1 (binding energy > -4.25 kcal mol^{-1}).The four ginsenosides exhibited good binding activity with EGFR (binding energy ≤ -4.25 kcal mol^{-1}) (Fig. 5). Because the binding energy of Rk1 with EGFR was

Table 1
Differential metabolites contributed to group classification.

Metabolites	Regulations (Model vs. Control)	FC	p-value
Malic acid	↓	0.31	0.007
Fumaric acid	↓	1.37	0.038
Citric acid	↓	0.7	0.003
Cis-Aconitic acid	↓	0.85	0.048
Heptadecanoic acid	↓	0.67	0.010
Nonadecanoic acid	↓	0.30	0.010
Hydrocinnamic acid	↓	0.31	0.028
4-Hydroxyphenylpyruvic acid	↓	0.05	0.038
p-Hydroxyphenylacetic acid	↓	0.73	0.049
2-Phenylpropionate	↓	0.50	0.050
Suberic acid	↓	0.79	0.028
Valeric acid	↓	0.46	0.050
Stearic acid	↓	0.34	0.050
Butyric acid	↓	0.14	0.002
Acetic acid	↓	0.72	0.043
Isobutyric acid	↓	0.47	0.030
L-Tryptophan	↑	11.31	0.021
L-Histidine	↑	4.31	0.031
L-Leucine	↑	1.29	0.0402
L-Glutamic acid	↑	3.03	0.012
L-Proline	↑	1.58	0.024
Glutathione	↓	0.69	0.037
3-Indoleacetonitrile	↓	0.54	0.05
Metabolites	Regulations (Model vs. GS)	FC	p-value
Citric acid	↓	0.76	0.046
Malic acid	↓	0.55	0.024
L-Glutamic acid	↑	1.30	0.028
Stearic acid	↓	0.23	0.010
Succinic acid	↓	0.69	0.023
Aconitic acid	↓	0.51	0.034
Heptadecanoic acid	↓	0.48	0.002
Pentadecanoic acid	↓	0.57	0.002
Hydroxypropionic acid	↓	0.26	0.028
Arachidic acid	↓	0.41	0.002
2-Phenylpropionate	↓	0.22	0.005
3-Indoleacetonitrile	↓	0.79	0.029
Butyric acid	↓	0.69	0.033
Tetracosanoic acid	↓	0.42	0.005
Valeric acid	↓	0.42	0.045
L-Tryptophan	↑	2.27	0.041
Behenic acid	↓	0.52	0.002

smallest(binding energy = −5.6 kcal mol^{-1}), futher study was designed to demonstrate the results of molecular docking.

3.7. EGFR target identification of ginsenoside Rk1 by CETSA

The CETSA method was used to study the affinity of ginsenoside Rk1 with intracellular EGFR. As shown in Fig. 6A, ginsenoside Rk1 increased the thermal stability of EGFR protein from 50 °C to 54 °C. At each temperature, the binding energy of the Rk1 group was greater than that of the DMSO group (Fig. 6B). CETSA indicated that ginsenoside Rk1 can bind to EGFR on Caco-2 cell membrane and stabilize its structure. The results of CETSA were consistent with the results of molecular docking. It was further demonstrated that ginsenoside Rk1 exerts anti-inflammatory effects by targeting EGFR.

4. Discussion

In the present study, the chemical composition of GS was first analyzed using LC-MS, which identified 10 ginsenosides. After the intragastric administration of GS to rats, it was observed that GS significantly increased the body weight, food consumption and decreased bloody stool, anus prolapse, dull hair and mental malaise of the model rats, in addition to alleviating the intestinal inflammation. In the inflammatory phase, the chronic accumulation of activated neutrophils, macrophages, and dendritic cells in the colonic mucus is accompanied by the release of cytokines TNF-α and IL-lβ [14]. In the present study, compared to the model group, the GS administration group had significantly decreased levels of TNF-α and IL-1 β in the serum ($P < 0.05$ and 0.01). Interleukin 10 is an inhibitor of cytokine synthesis and is involved in the inhibition of the secretion of proinflammatory cytokines via binding to their receptors [15]. GS treatment in the present study was observed to restore the acetic acid-decreased levels of IL-10.

Alterations in the gut microbiota are associated with the pathogenesis of various diseases, particularly inflammatory intestinal diseases [16]. In the present study, GS was observed to regulate the diversity and composition of gut microbiota in acetic acid-induced model rats, as evidenced by the Alpha diversity index (Chao1 and Shannon) and the distinct clustering in the PLS-DA analysis (Fig. 3A). Furthermore, the metabonomics analysis was conducted to explore the pharmacodynamic mechanism underlying the effect of GS in the treatment of IBD. The results revealed that there were 7 kinds of metabolites in the intestinal contents of the IBD model rats after the GS intervention, namely, acetic acid, butyric acid, citric acid, tryptophan, histidine, alanine, and glutathione. An elevated level of amino acid was observed in Model rats due to the malabsorption caused by intestinal inflammation, whereas a decreased the amount of SCFAs in Model group, such as acetic acid, propionic acid, butyrate and isobutyrate, seem to be the consequence of an

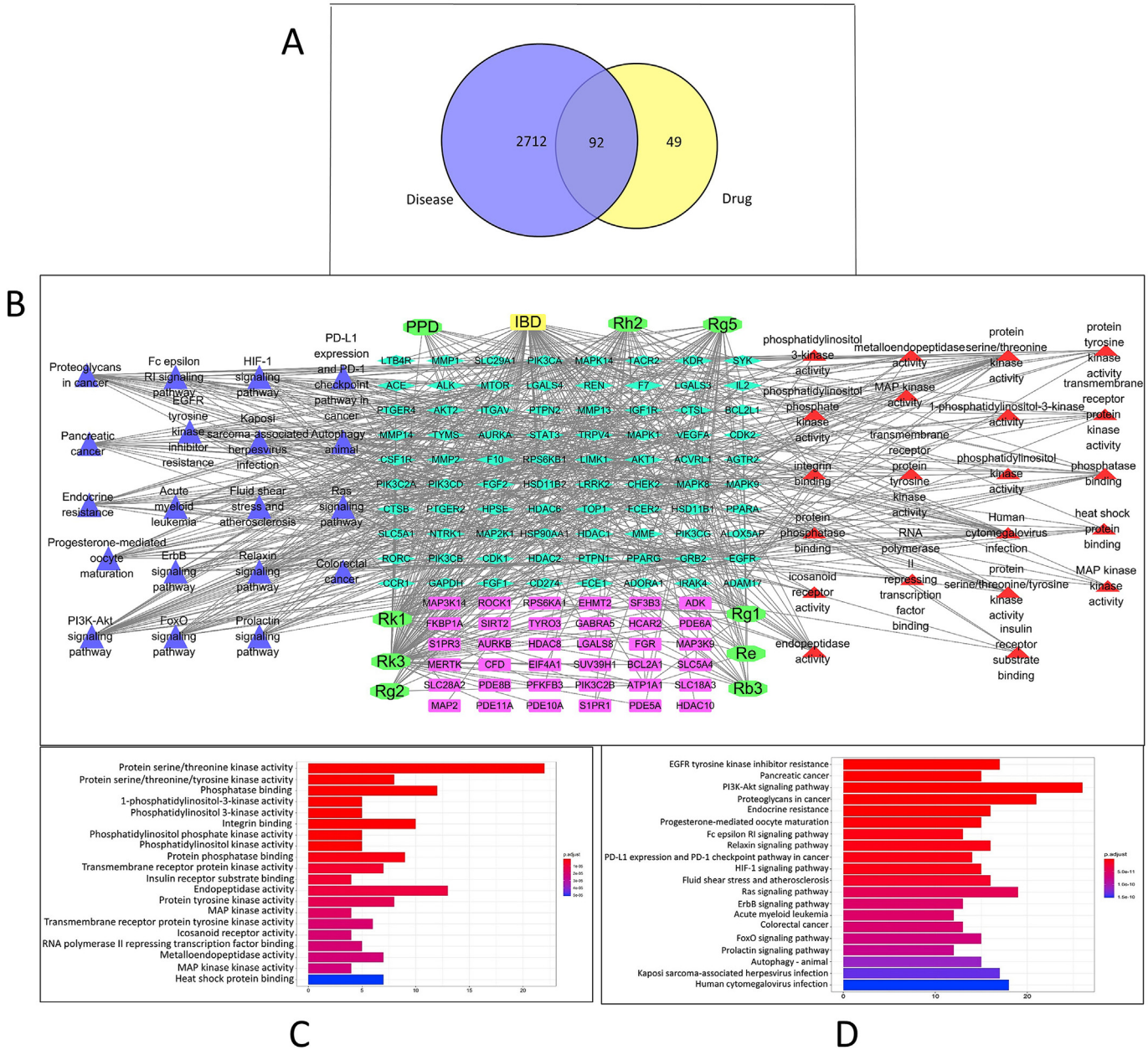

Fig. 4. Analysis of network pharmacology results of GS in the treatment of IBD. (A). The intersection result of disease target and drug target. (B). Component-protein target network; component-intersection target-pathway network and component-intersection target-biological function network. (C). Bar graph of GO analysis. (D). Bar graph of KEGG analysis.

Table 2
The number of intersection targets.

Compound	Intersection targets number
ginsenoside Rk3	63
ginsenoside Rk1	40
ginsenoside Rg5	27
ginsenoside Rh2	26
ginsenoside Rb3	13
ginsenoside Rg1	13
PPD	12
ginsenoside Re	10
ginsengoside Rg2	10

inflammation-driven intestinal dysbiosis [9,17]. These metabolites are mainly involved in the biosynthesis of SCFAs, TCA cycle, Ala and glutamate metabolism, histidine metabolism, and glutathione metabolism pathways. It was inferred that GS plays an important role in the IBD treatment by regulating and intervening with these potential metabolic markers and pathways. Glutathione (GSH) is an important antioxidant. The intestinal inflammation and mucosal damage occurring in inflammatory bowel disease are closely associated with the imbalance of redox and GSH contents [18]. Interestingly, according to the gut microbiota data of the present study, the amino acid metabolism-related bacteria, such as *Peptostreptococcaceae*, *Jeotgalicoccus*, *Corynebacterium*, and *Coprococcus*, demonstrated significant differences between the acetic acid-induced and control groups [19–21]. GS treatment could reverse these changes to different degrees. It is generally recognized that SCFAs, particularly acetic acid and butyric acid, are associated with sodium and fluid absorption and exert proliferative

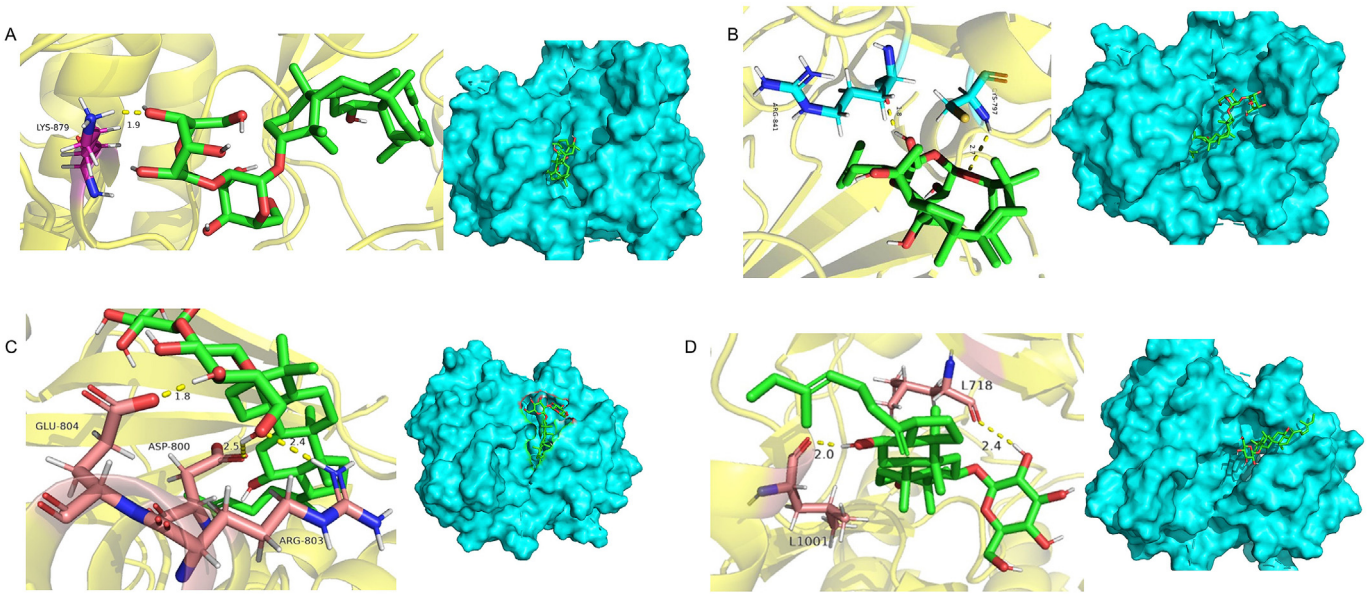

Fig. 5. Molecular docking results of 4 ginsenosides and EGFR protein. (A).Results of molecular docking between Rg5 and EGFR. Cartoon picture on the left. (B). Results of molecular docking between Rh2 and EGFR. (C). Results of molecular docking between Rk1 and EGFR; (D). Results of molecular docking between Rk3 and EGFR.

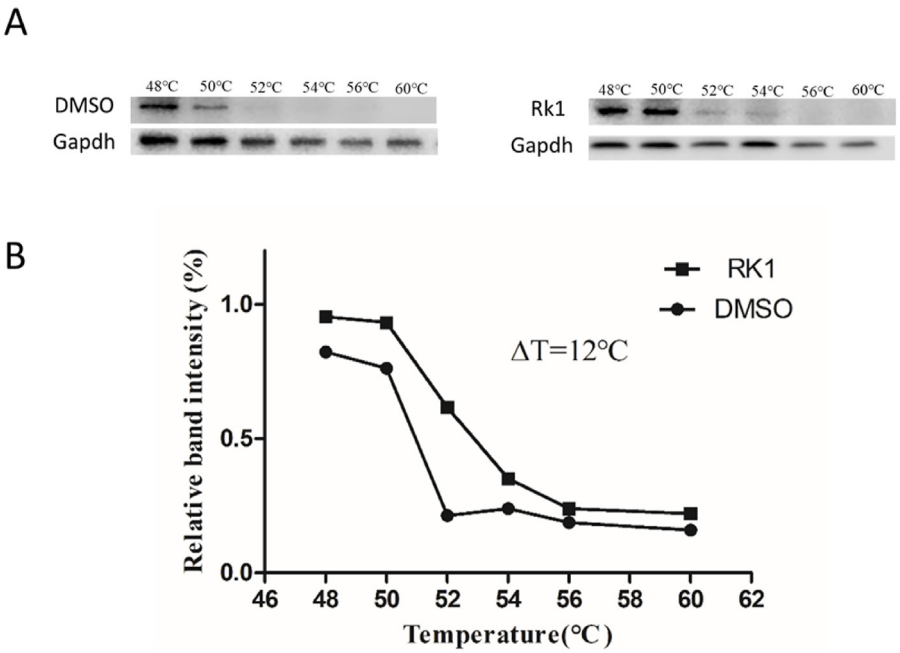

Fig. 6. The CETSA of Rk1with EGFR protein. (A). The presence of EGFR was analyzed by Western blotting. (B). EGFR expression were quantified by densitometry and plotted against temperature.

effects on colonocytes [22]. Therefore, acetic acid, butyric acid, and glutathione were selected as the potential metabolic markers in the present study, which is consistent with a large number of previously reported studies [9,17].

The results of network pharmacology revealed that the mechanism underlying the alleviating effect of ginsenosides in IBD might be closely associated with cell proliferation and differentiation, material metabolism, oxidative respiration, and energy metabolism pathways. Furthermore, EGFR, STAT3, and AKT1 were observed to be participating in most of the pathways. It was showed that the same pathway was connected to two or more targets, and the same target was related to different pathways, which indicated that the anti-colitis effect of ginsenosides could be the collective result of several pathways. For instance, AKT1 participates in 18 pathways and 4 biological activities, and the drugs targeting AKT1 might affect these pathways and biological activities simultaneously (Fig. 4B). GO and KEGG analyses showed the 92 intersection targets were observed to be involved in the EGFR tyrosine kinase inhibitor resistance, pancreatic cancer, PI3K-Akt signaling pathway, proteoglycan, endocrine resistance, AGE-RAGE signaling pathway, Ras signaling pathway, HIF-1 signaling pathway, FoxO Signal pathways, and other pathways (Fig. 4C). These pathways are mainly associated

with cell proliferation and differentiation, material metabolism, and oxidative respiration [23,24]. Next, the four ginsenosides RK1, rk3, Rg5, and Rh2, which presented higher scores for the degree values ($\geq$10), were used for molecular docking with EGFR, STAT3, and AKT1. The results revealed that the binding energy of these four ginsenosides to EGFR was low (binding energy ≤ -4.25 kcal mol^{-1}). It was speculated that EGFR could be the potential target for ginsenosides in their effect of improving IBD. These findings would guide future experimental research in this regard.

In conclusion, the combination of the analysis strategies of genomics, metabolomics, and network pharmacology used in the present study provides a novel approach to conduct research on natural products. The results of the present study demonstrated that ginseng has a great application value as a natural medicine in the treatment of IBD. Nonetheless, further research results and clinical data are required to support the clinical application of ginseng.

Funding

This work was supported by the National Key Research and Development Program of China [2017YFC1702100], the National Natural Science Foundation of China [81603276, U19A2013 and 82004099], the Department of Science and Technology of Jilin Province [20190101010JH, 20200201419JC and 202002053JC], and the Science and Technology Projects in Jilin Province Department of Education [JJKH20200903KJ]. Key Laboratory of Active Substances and Biological Mechanisms of Ginseng Efficacy, Ministry of Education. Jilin Provincial Key Laboratory of Bio-Macromolecules of Chinese Medicine.

Declaration of competing interest

The authors declare no conflict of interest.

Appendix A. Supplementary data

Supplementary data to this article can be found online at https://doi.org/10.1016/j.jgr.2022.04.001.

References

[1] Salvatori F, Siciliano S, Maione F, Esposito D, Masone S, Persico M, et al. Confocal Laser Endomicroscopy in the study of colonic mucosa in IBD patients: a Review, vol. 2012; 2012. p. 525098.
[2] Ananthakrishnan, Ashwin N, Bernstein, Charles N, et al. Environmental triggers in IBD: a review of progress and evidence. 2018.
[3] Shuai SA, Dwb C, Wei ZB, Xlb C, He Z, Dzb C, et al. A unique polysaccharide from Hericium erinaceus mycelium ameliorates acetic acid-induced ulcerative colitis rats by modulating the composition of the gut microbiota, short chain fatty acids levels and GPR41/43 respectors - ScienceDirect71; 2019. p. 411–22.
[4] Wijeyesekera A, Clarke PA, Bictash M, Brown IJ, Fidock M, Ryckmans T, et al. Quantitative UPLC-MS/MS analysis of the gut microbial co-metabolites phenylacetylglutamine, 4-cresyl sulphate and hippurate in human urine, vol. 4. INTERMAP Study; 2012.
[5] Yun M, Yi YS. Regulatory roles of ginseng on inflammatory caspases, executioners of inflammasome activation. J Ginseng Res 2020;44(3).
[6] Ji HK, Yi YS, Kim MY, Cho JY. Role of ginsenosides, the main active components of Panax ginseng, in inflammatory responses and diseases. J Ginseng Res 2017;41(4):435–43.
[7] Kim J-H. Cardiovascular diseases and Panax ginseng: a review on molecular mechanisms and medical applications. J Ginseng Res 2012;36(1):16–26.
[8] Liu J, Li T, Wang J, Zhao C, Geng C, Meng Q, et al. Different absorption and metabolism of ginsenosides after the administration of total ginsenosides and decoction of Panax ginseng. Rapid Commun Mass Spectrom 2020;34(13): e8788.
[9] Kaija-Leena K, Alberto P, Tytti J, De VWM, VJJoC Vidya, Colitis. Faecal and serum metabolomics in paediatric inflammatory bowel disease. J Crohn's Colitis 2017;(3):321–34.
[10] Wang J, Hou Y, Jia Z, Xie X, Liu J, Kang Y, et al. Metabonomics approach to comparing the anti-stress effects of four Panax ginseng components in rats. 2018. acs.jproteome.7b00559.
[11] Zovko A, Novak M, Håag P, Kovalerchick D, Holmlund T, Färnegårdh K, et al. Compounds from the marine sponge Cribrochalina vasculum offer a way to target IGF-1R mediated signaling in tumor cells. Oncotarget 2016;7(31): 50258–76.
[12] Zhang X, Xu H, Bi X, Hou G, Liu A, Zhao Y, et al. Src acts as the target of matrine to inhibit the proliferation of cancer cells by regulating phosphorylation signaling pathways. Cell Death Dis 2021;12(10):931.
[13] Wang L, Tang L, Feng Y, Zhao S, Han M, Zhang C, et al. A purified membrane protein from Akkermansia muciniphila or the pasteurised bacterium blunts colitis associated tumourigenesis by modulation of CD8+ T cells in mice. 2020. gutjnl-2019-320105.
[14] Nielsen Oh Jr E, Jess T. Safety of TNF-α inhibitors during IBD pregnancy: a systematic review. BMC Med. 2013;11(1):174.
[15] Melgar S, Yeung MW, Bas A, Forsberg G, Hammarstrom MLJC, Immunology E. Over-expression of interleukin 10 in mucosal T cells of patients with active ulcerative colitis134; 2003. p. 127–37. 1.
[16] Sangild PT. Development of the mammalian gastrointestinal tract, the resident microbiota, and the role of diet in early life3; 2011. p. 85. 3.
[17] Bjerrum JT, Wang Y, Hao F, Coskun M, Ludwig C, Günther U, et al. Metabonomics of human fecal extracts characterize ulcerative colitis, Crohn's disease and healthy individuals. Metabolomics 2015;11(1):122–33.
[18] Kumari R, Ahuja V, Paul J. Fluctuations in butyrate-producing bacteria in ulcerative colitis patients of North India. World J Gastroenterol 2013;(22): 39–49.
[19] Sun ML, Kim N, Yoon H, Yong SK, Dong HLJG, Liver. Compositional and functional changes in the gut microbiota in irritable bowel syndrome patients. 2020.
[20] Liu ZX, Chen J, Tang SK, Zhang YQ, He JW, Chen QH, et al. Jeotgalicoccus nanhaiensis sp. nov., isolated from intertidal sediment, and emended description of the genus Jeotgalicoccus61; 2011. p. 2029. 9.
[21] Kirchner O, AJJoB Tauch. Tools for genetic engineering in the amino acid-producing bacterium. Corynebacterium glutamicum 2003;104(1–3):287–99.
[22] Mamiko Kobayashi, Daisuke Mikami, Hideki Kimura, et al. Short-chain fatty acids, GPR41 and GPR43 ligands, inhibit TNF-α-induced MCP-1 expression by modulating p38 and JNK signaling pathways in human renal cortical epithelial cells. 2017.
[23] Zhang F, Zhen-Lu LI, Xiao-Mei XU, Yan HU, Yao JH, Wei XU, et al. Protective effects of icariin-mediated SIRT1/FOXO3 signaling pathway on intestinal ischemia/reperfusion-induced acute lung injury11; 2015. p. 269–76. 1.
[24] Pothoulakis Charalabos, Xue Xiang, Bakirtzi Kyriaki, et al. Neurotensin promotes the development of colitis and intestinal angiogenesis via Hif-1 alpha-miR-210 signaling. 2016.